AUTONOMOUS RELATIVE NAVIGATION FOR FORMATION-FLYING SATELLITES USING GPS

Cheryl GRAMLING and J. Russell CARPENTER
NASA Goddard Space Flight Center
Greenbelt, Maryland USA 20771

Anne LONG, David KELBEL, and Taesul LEE
Computer Sciences Corporation
Lanham-Seabrook, Maryland USA 20706

ABSTRACT *– The Goddard Space Flight Center is currently developing advanced spacecraft systems to provide autonomous navigation and control of formation flyers. This paper discusses autonomous relative navigation performance for a formation of four eccentric, medium-altitude Earth-orbiting satellites using Global Positioning System (GPS) Standard Positioning Service (SPS) and "GPS-like" intersatellite measurements. The performance of several candidate relative navigation approaches is evaluated. These analyses indicate that an autonomous relative navigation position accuracy of 1 meter root-mean-square can be achieved by differencing high-accuracy filtered solutions if only measurements from common GPS space vehicles are used in the independently-estimated solutions.*

1 – INTRODUCTION

Formation-flying techniques and satellite autonomy will revolutionize space and Earth science missions and enable many small, inexpensive satellites to fly in formation and gather concurrent science data. The Guidance, Navigation, and Control Center (GNCC) at Goddard Space Flight Center (GSFC) has successfully developed high-accuracy autonomous satellite navigation systems using the National Aeronautics and Space Administration's space and ground communications systems and the Global Positioning System (GPS) [Gram 94, Hart 97]. Recently, the GNCC has leveraged this experience to develop advanced spacecraft systems that provide autonomous navigation and control of formation flyers.

To support this effort, the GNCC is assessing the absolute and relative navigation accuracy achievable for proposed formations using GPS and "GPS-like" intersatellite measurements. Several universities and corporations are developing GPS transceivers that support this tracking concept for NASA and the Air Force Research Laboratory; these include Johns Hopkins Applied Physics Laboratory, International Telephone and Telegraph, Honeywell, Motorola, Jet Propulsion Laboratory, Cincinnati Electronics, and Stanford University [Baue 99].

Published flight data results ([Braz 96], [Schi 98], [More 98], [Kama 99]) have shown relative orbit determination performance at the meter- to decameter-level using relative GPS pseudorange data for rendezvous and docking scenarios in low Earth orbits. This paper addresses the level of relative navigation performance achievable for a different class of missions, i.e. more than two vehicles maintaining a relatively tight formation, in a relatively ecentric orbit.

This class of missions is represented by a tetrahedral formation designed to support a proposed mission to study the Earth's aurora. This formation consists of four satellites maintained in eccentric Earth orbits of approximately 500 by 7000 kilometer altitudes, with initial separations of 10 to 30 kilometers. Maneuvers would be performed monthly to maintain this configuration. To

support autonomous planning of these maneuvers, the total relative position and velocity accuracy must be about 100 meters and 2 centimeters per second, respectively. Later in the mission, the separation would be reduced to about 500 meters, which would reduce the total relative position accuracy requirements to about 5 meters. This paper quantifies the relative navigation accuracy achievable for this formation by differencing satellite state vectors that are independently estimated using either a geometric point solution method or a high-accuracy extended Kalman filter.

2 – RELATIVE NAVIGATION CONCEPTS

The most straightforward relative navigation approach computes the satellite relative positions by differencing the absolute position vectors of each satellite in the formation [Zyla 93]. The state differencing method can be used to support decentralized, centralized, or hierarchical formation control strategies. Fig. 1 illustrates a possible concept for using this approach to support decentralized control of a distributed satellite formation. In this case, each satellite independently computes its absolute state vector using GPS and possibly "GPS-like" intersatellite measurements and transfers it via an intersatellite communications link to every other satellite in the formation. Each satellite computes its relative position to the other satellites by state vector differencing and uses this relative state to plan and execute formation maintenance maneuvers to maintain its desired position within the formation. [Carp 00] discusses a recent investigation of decentralized formation control strategies.

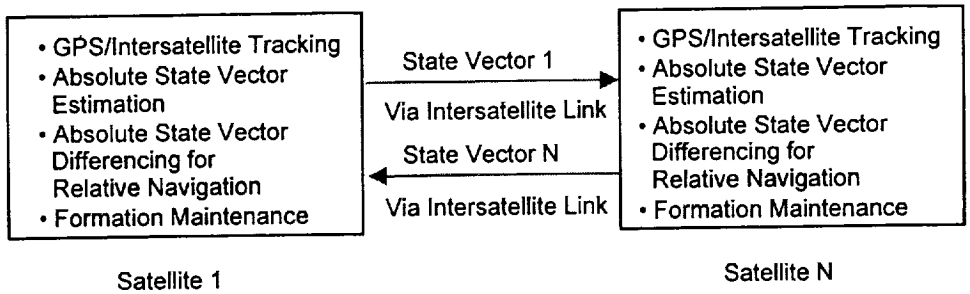

Fig. 1 State Vector Differencing Configuration with Decentralized Formation Control

The absolute state vector computation can be performed using either an instantaneous point solution method or a real-time filtered algorithm. The typical GPS Standard Positioning Service (SPS) receiver computes the real-time three-dimensional spacecraft position and receiver time bias by solving a set of simultaneous equations constructed using pseudorange measurements to a minimum of four GPS space vehicles (SVs). These products are often referred to as geometric or point solutions. The major sources of error in the GPS SPS measurements arise from uncorrected ionospheric delays and the Selective Availability (SA) corruption applied to the GPS signals and ephemerides to limit geometric solutions to approximately 100 meters (two-dimensional, 95 percent of the time) when SA is enabled. Typically, GPS receiver vendors advertise three-dimensional position accuracy on the order of 150 meters (1σ).

A real-time filtered algorithm, such as that implemented in the GPS Enhanced Orbit Determination (GEODE) software [Godd 00], reduces the impact of the measurement errors by using an extended Kalman filter in conjunction with a high-fidelity orbital dynamics model. In addition to the simple state vector differencing approach, the real-time filtered approach can support the following increasingly more complex relative navigation approaches

- Simultaneous estimation of the local and remote satellites using singly-differenced GPS measurements between the local and remote satellites
- Simultaneous estimation of the local and remote satellites and GPS SV measurement biases using GPS measurements from all satellites
- Simultaneous estimation of the local and remote satellites using GPS measurements to all satellites and "GPS-like" measurements between the local and remote satellites

It is anticipated that the more complex approaches will provide more accurate relative navigation solutions (for example, see [Axel 86], [Gald 93], [Zyla 93], [Binn 97], [Cora 98]).

3 – PERFORMANCE SIMULATION PROCEDURE

The formation studied consists of four satellites maintained in eccentric Earth orbits at an inclination of 80 degrees with altitudes of approximately 500 kilometers at perigee by 7000 kilometers at apogee. All satellites have nearly identical surface areas of 0.6613 meters^2 and masses of 200 kilograms. Each satellite is offset from the other satellites by a total of approximately 10 to 30 kilometers, in and/or out of the orbit plane, forming a tetrahedron. To quantify the level of absolute and relative navigation performance that is achievable, GPS and "GPS-like" intersatellite measurements were simulated for the two satellites that are in the same orbital plane and used to estimate their absolute and relative positions and velocities.

Realistic GPS pseudorange and "GPS-like" intersatellite measurements were simulated for each satellite based on truth ephemerides computed using the Goddard Trajectory Determination System (GTDS), which is the primary orbit determination program used for operational satellite support at GSFC. The truth ephemerides were computed using a high-fidelity force model that included a 70 by 70 Joint Goddard Model (JGM)-2 for nonspherical gravity forces, Jet Propulsion Laboratory Definitive Ephemeris 200 for solar and lunar gravitational forces, a Harris-Priester atmospheric density model, and solar radiation pressure forces. Table 1 lists the measurement simulation options.

Table 1. Measurement Simulation Parameters

Parameter	Value
Measurement data rate	GPS: Every 1 minute from all visible GPS SVs Intersatellite: Every 3 minutes from each transmitting satellite
GPS SV ephemerides	Broadcast ephemerides for July 19-22, 1998
GPS signal characteristics: SA errors Transmitting antenna pattern Transmitted power	 25 meter (1-sigma) GPS L-band pattern, modeled from 0 to 90 degrees down from boresight 28 dB-Watts in maximum gain direction
User antenna models:	Hemispherical GPS antenna: anti-nadir pointing Maximum gain : 4.9dBic Horizon mask: 85 degrees from boresight
Visibility constraints	• Earth blockage with 50 km altitude tropospheric mask • GPS SV transmitting antenna main beam and receiving antenna horizon masks • No constraints on intersatellite link
Receiver characteristics	• 9 channels for GPS • 3 channels for intersatellite link • 35 dB-Hertz receiver acquisition threshold
Receiver clock bias white noise spectral density	9.616×10^{-20} seconds^2 per second
Receiver clock drift rate white noise spectral density	1.043×10^{-27} seconds^2 per seconds^3
Random measurement errors	GPS pseudorange: 2 meters (1-sigma) Intersatellite pseudorange: 3 meters (1-sigma)
Ionospheric delays	21.3 meters at 500 kilometer height 3.4 meters at 1000 kilometer height

The GPS constellation configuration was based on the GPS broadcast messages for the epoch date and the GPS signal strength at the GPS receiver's location was modeled assuming the nominal GPS Block II signal antenna pattern (including both the main and side lobes). Each user satellite had one hemispherical GPS antenna, with boresight anti-nadir pointing. The GPS receiver's acquisition threshold was set at 35 dB-hertz, consistent with the performance of most space receivers. The GPS SV signal attenuation model that was used provides realistic signal acquisition predictions [More

99]. The number of simultaneous measurements was limited to nine GPS (selected based on highest signal-to-noise ratio) and three intersatellite, consistent with the use of a twelve-channel GPS transreceiver. No constraints were placed on acquisition of the intersatellite signal.

Fig. 2 shows the number of GPS SVs visible as a function of time and altitude. The satellites' single hemispherical antenna considerably limits GPS visibility at high altitudes. The periods of lowest visibility (4 or fewer) occur when the satellites are at altitudes above 5500 kilometers, where the visibility is highly dependent on the exact position of the GPS SVs within each orbit plane. The periods of best visibility with 6 or more visible GPS SVs occur when the satellites are within the main lobe of the GPS signal (i.e. below approximately 3000 kilometers).

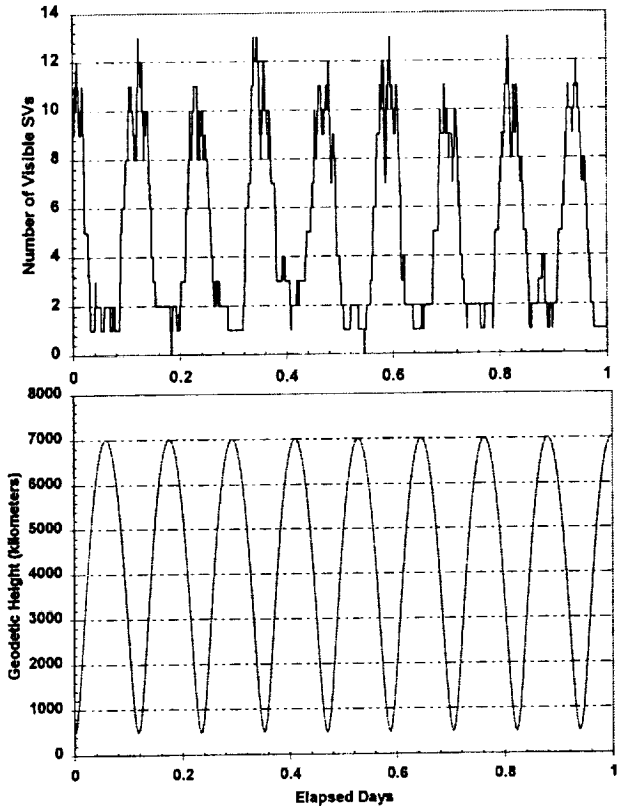

Fig. 2. GPS SV Visibility as a Function Time and Altitude

Selective Availability (SA) errors were applied to the GPS measurements at a 25-meter (1-sigma) level, using the Lear4 autoregressive integrated moving average time series model [JSC 93]. This model was used with a 2-meter (1-sigma) error level to model the residual SPS ephemeris and clock errors when SA is disabled, which is expected by 2005. Ionospheric delays were modeled as a function of the height of the signal path above the Earth, which was based on ionospheric delays computed for the test orbit using the Bent ionospheric model available in GTDS. Receiver clock noise was simulated assuming a highly-stable crystal oscillator with a 1-second root Allan variance of $0.16(10^{-9})$. A twice-integrated random walk model, which is based on [Brow 97], was used to simulate the clock bias and clock drift noise contributions to the GPS measurement errors.

To minimize potentially large biases in the intersatellite measurements, each transmitting satellite would estimate its clock offset from GPS time and frequency offset from nominal based on GPS measurements and steer its clock to be synchronized to within 100 nanoseconds (30 m) with GPS time. Each transmitting satellite would transmit a pseudorandom noise (PN) code starting at the whole millisecond, synchronized with GPS Time to within the accuracy of its clock offset estimate. Alternately, the transmitting satellite could provide its clock offset and frequency bias estimates as part of its navigation message and these biases could be included in the measurement model. The expected intersatellite pseudorange measurement biases in the transmitter and receiver clock offset estimates were not included in the preliminary analysis reported in this paper.

The GPS pseudorange measurement sets were processed using both the point solution method and the real-time filtered algorithm that is available in the GEODE flight software. GEODE was also used to process measurement sets that included intersatellite measurements. The absolute navigation errors were computed by differencing the truth and estimated absolute state vectors. The estimated relative state vectors were computed by differencing the estimated absolute state vectors for the two satellites. The relative navigation errors were computed by differencing the true relative state vectors and the estimated relative state vectors.

4 – RELATIVE NAVIGATION PERFORMANCE BY DIFFERENCING POINT SOLUTIONS

This section presents the absolute and relative navigation results obtained using the point solution method for computation of the absolute state vectors. The point solution method provides the absolute position vector and receiver clock bias for each satellite at every measurement time for which a minimum of four GPS measurements is available. This method uses all available GPS pseudorange measurements from up to a maximum of nine GPS SVs.

The left-hand side of Fig. 3 shows the absolute root-mean-square (RMS) and maximum position errors of the point solutions with and without SA enabled, when six or more GPS SVs are visible. The left-hand side of Fig. 4 shows the absolute point solution position error versus time for a representative set of individual point solutions with SA enabled. Using a single anti-nadir pointing antenna, there are periods of about 70 minutes every orbit when fewer than four measurements are available and point solutions cannot be computed. With or without SA enabled, the peak absolute errors of more than 1 kilometer occur for solutions near apogee, where the number of visible satellites is five or fewer and the geometrical distribution is poor. During periods of good visibility (i.e. six or more visible GPS SVs), the absolute radial, in-track, and cross-track (RIC) RMS position errors are 47 meters, 20 meters and 17 meters, respectively. Elimination of the SA-induced GPS ephemeris and clock errors significantly reduces the absolute RIC RMS position errors to about 19 meters, 5.4 meters and 4.5 meters, respectively.

This point solution method does not provide absolute velocity solutions directly. The absolute velocity vectors were computed by differentiating a quadratic polynomial fit to the four nearest position vectors, computed at a 1-second spacing. This produced RMS velocity errors of approximately 10 meters per second during periods with 6 or more visible GPS SVs, with significantly larger errors when fewer than 6 GPS SVs are visible.

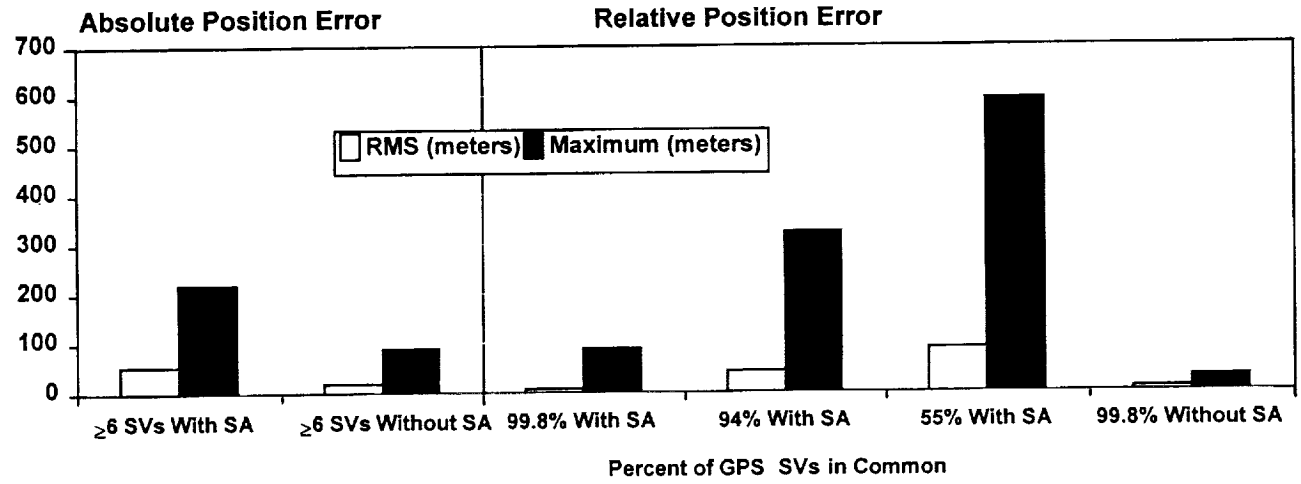

Fig. 3. Absolute and Relative Satellite Position Errors Using Point Solutions With Six or More Visible GPS SVs

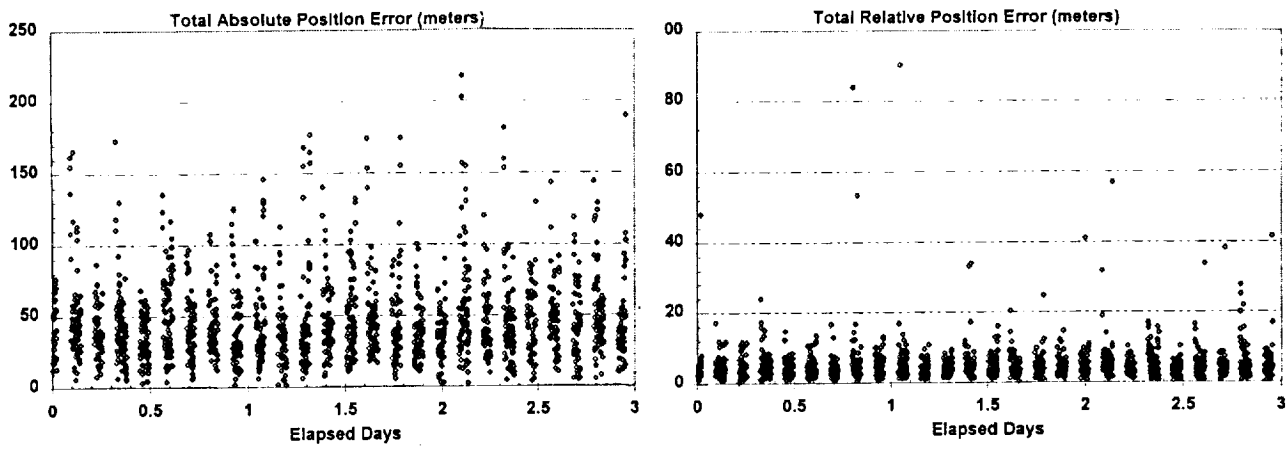

Fig 4. Absolute and Relative Satellite Position Errors With SA Enabled Using Point Solutions

The right-hand side of Fig. 3 summarizes the relative solution errors obtained by differencing the absolute point solutions for each satellite with six or more visible GPS SVs, varying the percentage of measurements from common GPS SVs. The right-hand side of Fig. 4 shows the relative point solution position error versus time when the percentage of common GPS SVs is high (99.8% with SA). In this case when the absolute solutions are differenced, the solution error contributions from correlated measurement errors (due primarily to SA and ionospheric delay) cancel and the relative navigation error is significantly smaller than the absolute error. When the percentage of common GPS SVs used by each satellite decreases, less of the solution error contribution from measurement error is correlated. In these cases when the absolute solutions are differenced, error cancellation is significantly less. The largest relative navigation error would occur if the absolute point solutions were computed using measurement sets that are not from common GPS SVs. In this case, the relative navigation errors would equal the root sum square of the individual absolute position errors.

When the absolute solutions obtained without SA are differenced, cancellation of the remaining correlated absolute solution errors (primarily due to ionospheric delay errors) is less than when SA is enabled but still significant. The relative position RMS error without SA (6 meters) is nearly identical to the relative position RMS error with SA enabled (7 meters), when only common SVs are used in the computation of the absolute state vectors.

5 – RELATIVE NAVIGATION PERFORMANCE BY DIFFERENCING FILTERED SOLUTIONS

This section presents the absolute and relative navigation results obtained using a real-time filtering algorithm for computation of the absolute state vectors. The extended Kalman filter algorithm available in the GEODE flight software was used to process the GPS pseudorange measurement sets, as well as measurement sets that included intersatellite measurements. Table 2 lists the GEODE processing parameters. Atmospheric drag and solar radiation pressure forces were included in the state propagation using atmospheric drag and solar radiation pressure coefficients that were offset by 10 percent and 3 percent respectively from the values used in the truth ephemeris generation. A Monte Carlo error analysis was performed. Ensemble error statistics were accumulated for absolute and relative navigation solutions obtained by processing 50 sets of simulated pseudorange measurements that were created by the varying the random number seeds for the SA, random, and clock measurement errors.

The left hand side of Fig. 5 compares the steady-state time-wise ensemble true RMS and maximum errors of the absolute position estimates, with and without SA enabled. The ensemble true RMS/maximum error is the RMS/maximum of the true error (difference between the estimated and the true state) at each time computed across all 50 Monte Carlo solutions. The steady-state time-wise ensemble true RMS/maximum error is the RMS/maximum along the time axis of the ensemble

true errors, omitting the initial convergence period (1 day). Figures 6 and 7 show the ensemble true RMS error of the absolute position and velocity estimates for representative cases with SA enabled and with SA disabled, respectively.

Table 2. GEODE Processing Parameters

Parameter	Value
Nonspherical Earth Gravity model	30x30 Joint Goddard Model (JGM)-2
Solar and lunar ephemeris	Low-precision analytical ephemeris
Initial position error in each component	100 meters
Initial velocity error in each component	0.1 meter per second
Atmospheric drag coefficient error	0.22 (10 percent)
Solar radiation pressure coefficient error	0.042 (3 percent)
Initial receiver time bias error	100 meters
Initial receiver time bias rate error	1 meter per second
Estimated state	• User position and velocity • GPS receiver time bias and time bias drift
GPS SV ephemerides	Broadcast GPS ephemerides for July 19-22, 1998
Intersatellite transmitter ephemerides	Real-time filtered solution for same period
Ionospheric editing	500 kilometer minimum height of signal path
Measurement processing rate	GPS: All available pseudoranges every 3 minutes Intersatellite: All available pseudoranges every 3 minutes

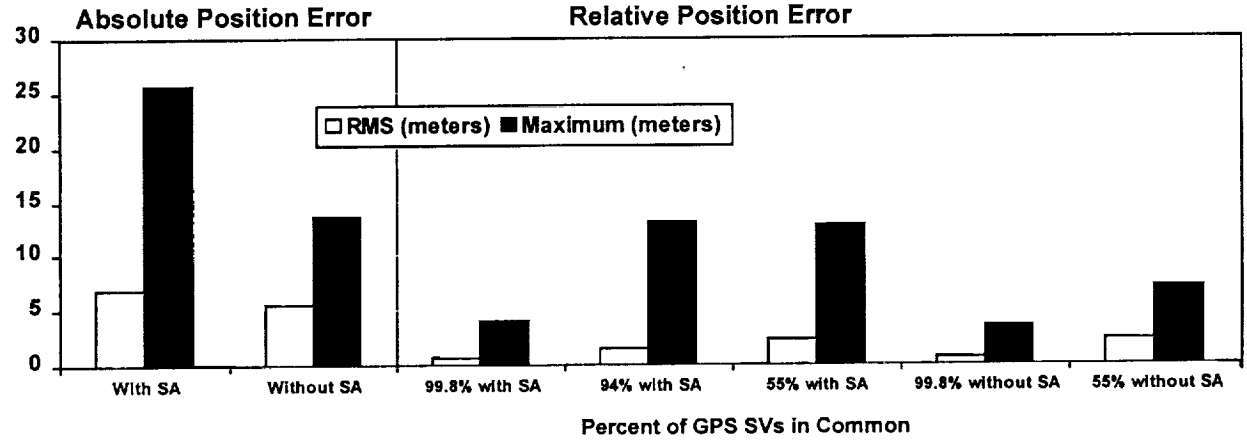

Fig. 5. Absolute and Relative Steady-State Time-Wise Ensemble True Position Errors Using Filtered Solutions with GPS Measurements

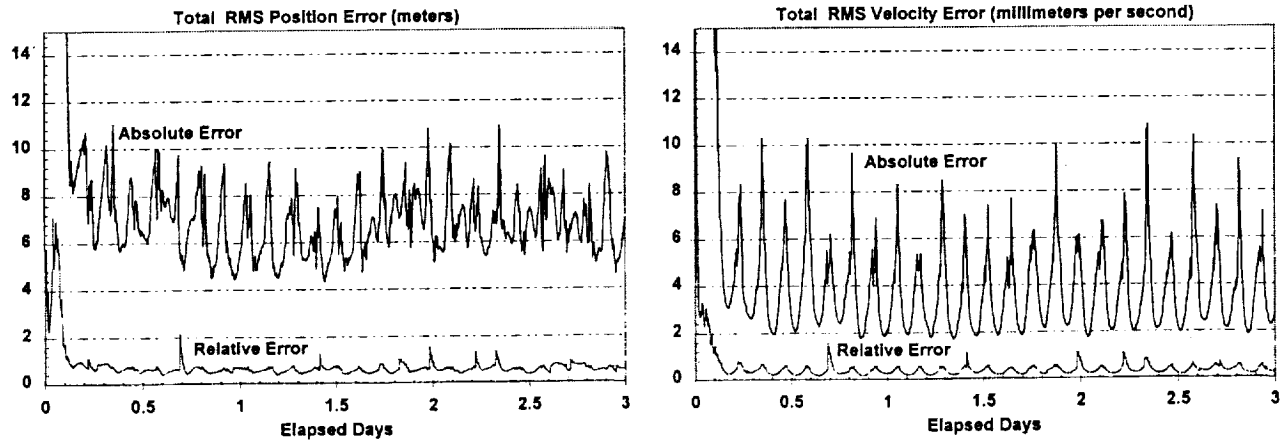

Fig 6. Absolute and Relative Ensemble True RMS Position and Velocity Errors With SA Enabled Using Filtered Solutions with 99.8% GPS SVs in Common

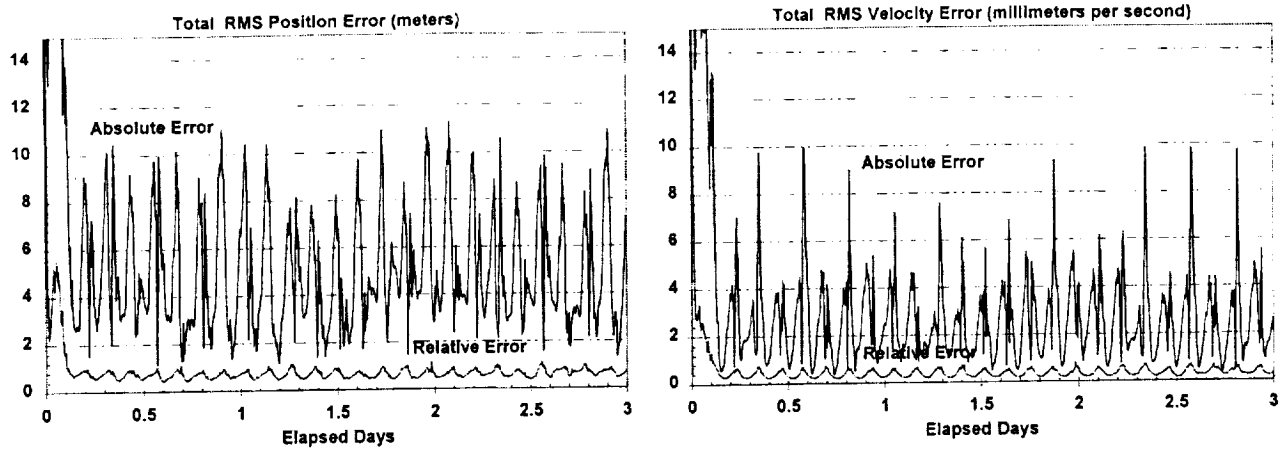

Fig 7. Absolute and Relative Ensemble True RMS Position and Velocity Errors With SA Disabled Using Filtered Solutions with 99.8% GPS SVs in Common

With SA enabled, the absolute filtered position errors are significantly smaller than the absolute point solution position errors shown in Fig. 2, with RIC RMS position errors of 2.6 meters, 5.9 meters, and 2.0 meters, respectively. The filtered solutions also provide reliable, high-accuracy velocity estimates with RIC RMS velocity errors of 3.6 millimeters per second, 1.4 millimeters per second, and 1.2 millimeters per second, respectively. The level of accuracy is consistent over the entire orbit, insensitive to the number of visible GPS SVs at any specific time. Elimination of the SA-induced GPS ephemeris and clock errors reduces the absolute RIC RMS position errors to approximately 2.8 meters, 4.5 meters and 1.3 meters, respectively.

The right hand side of Fig. 5 summarizes the relative solution errors obtained by differencing the absolute filtered solutions for each satellite. The lowest relative errors were obtained when the absolute filter processing was synchronized so that a high percentage of the measurements used to compute the absolute filter solutions were from common SVs (99.8% with SA), yielding RMS RIC relative position errors of 0.17 meters, 0.56 meters, and 0.17 meters, and RMS RIC relative velocity errors of 0.36 millimeter per second, 0.09 millimeter per second, and 0.1 millimeter per second, respectively. Fig. 6 also shows the relative ensemble true RMS position and velocity errors versus time when the percentage of common GPS SVs is high (99.8% with SA). In this case, when the absolute solutions are differenced, the error contributions from correlated measurement and dynamic errors cancel and the relative navigation accuracy is significantly better than the absolute errors. Since the satellites are in nearly the same orbits, the dynamic errors are highly correlated, and a large percentage of the dynamic error contribution cancels in all of these cases. When the percentage of common GPS SVs used by each satellite decreases, less of the measurement error is correlated. Consequently, the absolute error cancellation in the differenced solutions is less and relative errors increase as the percentage of common GPS SVs decreases. With SA disabled (99.8% without SA), the RMS relative position errors are comparable to the SA-enabled case with nearly complete satellite synchronization (99.8% with SA).

A preliminary assessment was made of the impact of augmenting the GPS pseudorange measurements with "GPS-like" intersatellite measurements. In the approach evaluated, the absolute state vector of the local satellite was estimated independently using GPS and intersatellite pseudorange measurements from the other satellites in the formation. This simulation assumed that a navigation message containing the absolute state vector of each of the transmitting satellites would be provided to the receiving satellite using the intersatellite communications link and used to model the intersatellite measurements and to compute the relative state vector by the state vector differencing method. When the ephemeris provided for each transmitting satellite was that obtained by estimation using only GPS measurements (with RMS position errors of about 8 meters), the absolute and relative solution errors are comparable to those obtained using only GPS measurements. When the true ephemeris of each transmitting satellite was provided, the absolute

solution error for the local receiving satellite decreased to below 2 meters but the relative navigation increased due to the reduction in the cancellation of the solution error contributions from correlated dynamic and measurement errors. These preliminary results indicate that high accuracy relative navigation solutions using cross-link measurements will require that cross-link measurements be included in the solutions for all the satellites in formation, in order to maximize the cancellation of the absolute error contributions.

6 – CONCLUSIONS AND FUTURE DIRECTIONS

This study assesses the feasibility of using state vector differencing for relative navigation. When SA is enabled, relative navigation accuracies of better than 10 meters RMS are achievable when six or more GPS SVs are mutually visible by differencing point solutions, if only measurements from GPS SVs common to both satellites are used in the absolute solutions. However, the use of point solutions is not suitable for continuous real-time navigation in configurations where fewer than six GPS SVs are visible during significant portions of the orbit. For the 500 by 7000 kilometer formation used in this study, reliable point solutions would be available only about 50 percent of the time using a single hemispherical antenna, improving to about 90 percent of the time using an omnidirectional antenna configuration. Because point solutions do not provide accurate velocity estimates, they are not suitable for applications in which state vector information must be predicted ahead in time, e.g., to support autonomous maneuver planning.

If the absolute state vectors are computed using a high-accuracy filter, the relative navigation accuracy improves to better than 1 meter and 0.5 millimeter per second RMS if only measurements from GPS SVs common to both satellites are used in the absolute solutions. This level of performance is maintained over the entire orbit, insensitive to the number of visible GPS SVs at any specific time. This relative accuracy satisfies the most stringent navigation requirements for autonomous maneuver planning of the formation studied. The relative accuracy degrades as the percentage of measurements from common GPS SVs that are used in the point solutions decreases. In formations for which the separation distances are less than 100 kilometers, such as the formation studied in this report, GPS SV visibility will be nearly identical for all user satellites. In this case, restricting the measurements processed to those from common GPS SVs is not unreasonable.

Future directions will initially focus on a detailed investigation of improvements to be realized through the simultaneous estimation of the local and remote satellite state vectors. Expectations are that the relative navigation performance will be improved through the processing of single-differenced measurements or the estimation of GPS-SV-related biases and the processing of intersatellite measurements to simultaneously estimate the location of all satellites in the formation. The GEODE flight software, which has recently been enhanced to support multiple satellite estimation and additional measurement types, will be used in these studies. The relative navigation version of GEODE is being integrated into a low cost GPS satellite receiver being developed by the GSFC GNCC. This formation-flying receiver will be used to demonstrate end-to-end performance in GNCC's formation-flying test bed.

REFERENCES

[Axel 86] P. Axelrad and J. Kelley, "Near Earth Orbit Determination and Rendezvous Navigation using GPS," *Proceedings of the 1986 IEEE Position Location and Navigation Conference*, November 1986, pp.184-191.

[Baue 99] F. Bauer et al., "Enabling Spacecraft Formation Flying Through Spacebourne GPS and Enhanced Autonomy Technology," *Proceedings of the ION GPS-99*, Nashville, TN, September 1999

[Binn 97] P. Binning, "Satellite to Satellite Relative Navigation Using GPS Pseudoranges," *Proceedings of the 1997 ION National Technical Meeting*, January 1997, pp.407-415.

[Braz 96] J. Brazzel, et al. "Flight Test Results from Real-Time Relative GPS Experiment on STS-69," *Space Flight Mechanics 1996*, AAS Publications Office, San Diego, CA

[Brow 97] R. G. Brown and P. Y. C. Hwang, *Introduction to Random Signals and Applied Kalman Filtering*, Third Edition, John Wiley and Sons, 1997

[Carp 00] J. R. Carpenter, "A Preliminary Invetigation of Decentralized Control for Satellite Formations," Paper 264 presented at the IEEE Aerospace Conference, Big Sky Montana, March 20-22, 2000

[Cora 98] T. Corrazini, et al., "Experimental Demonstration of GPS as a Relative Sensor for Formation Flying Spacecraft," *Navigation*, 45(3), pp.195-207.

[Gald 93] J. Galdos, et al., "A GPS Relative Navigation Filter for Automatic Rendezvous and Capture," *Proceedings of the 1993 ION National Technical Meeting*, January 1993, pp.83-94.

[Godd 00] Goddard Space Flight Center, CSC-96-968-01R0UD1, *Global Positioning System (GPS) Enhanced Orbit Determination (GEODE) Mathematical Specifications, Version 5*, T. Lee and A. Long (CSC), prepared by Computer Sciences Corporation, February 2000

[Gram 94] C. J. Gramling et al., "TDRSS Onboard Navigation System (TONS) Flight Qualification Experiment," *Proceedings of the Flight Mechanics/Estimation Theory Symposium 1994*, NASA Conference Publication 3265, May 17-19, 1994, pp.253-267

[Hart 97] R. Hart, A. Long, and T. Lee, "Autonomous Navigation of the SSTI/Lewis Spacecraft Using the Global Positioning System (GPS), *Proceedings of the Flight Mechanics Symposium 1997*, NASA Conference Publication 3345, May 19-21, 1997, pp.123-133

[JSC 93] Johnson Space Flight Center, *Range Bias Models for GPS Navigation Filters*, William M. Lear, Charles Stark Draper Laboratory, June 1993

[Kama 99] I. Kamano, et al. "Result and Evaluation of Autonomous Rendezvous Docking Experiment of ETS-VII," *Proceedings of the 1999 AIAA GN&C Conference*, Portland, OR, August 1999

[More 98] G. Moreau and H. Marcille, "RGPS Post-flight Analysis of ARP-K Flight Demonstrations," *Proceedings of the ION GPS-98*, Nashville, TN, September 1998

[More 99] M. Moreau et al., "GPS Receiver Architecture and Expected Performance for Autonomous GPS Navigation in Highly Eccentric Orbits," *Proceedings of the 55th Annual ION Meeting*, Cambridge Massachusetts, June 28-30, 1999

[Schi 98] E. Schiesser, et al. "Results of STS-80 Relative GPS Navigation Flight Experiment," *Space Flight Mechanics 1998*, AAS Publications Office, San Diego, CA

[Zyla 93] L. Zyla and M. Montez, "Use of Two GPS Receivers in Order to Perform Space Vehicle Orbital Rendezvous," *Proceedings of the ION-GPS-93*, September 1993, pp. 301-312